Theoretical analysis of interaction between a particle and an oscillating bubble driven by ultrasound waves in liquid*

Yao-Rong Wu(武耀蓉) and Cheng-Hui Wang(王成会)†

Institute of Applied Acoustics, Shaanxi Normal University, Xi'an 710062, *China*

(Received 1 June 2017; revised manuscript received 13 July 2017; published online 30 September 2017)

A theoretical model is developed to describe the interaction of a particle and an oscillating bubble at arbitrary separation between them. The derivation of the model is based on the multipole expansion of the particle and bubble velocity potentials and the use of Lagrangian mechanics. The model consists of three coupled ordinary differential equations. One of them accounts for the pulsation of the bubble and the other two describe the translation of the bubble and particle in an infinite, incompressible liquid. The model here is accurate to order $1/d^{10}$, where d is the distance between the centers of the particle and bubble. The effects of the size and density of the particle are investigated, namely, the interaction between the particle and bubble changes from repulsion to attraction with the increment of the particle density, and the increment of the particle size makes the interaction between the particle and bubble stronger. It is demonstrated that the driving frequency and acoustic pressure amplitude can affect the interaction of the particle and bubble. It is shown that the correct modeling of the translational dynamics of the bubble and particle at small separation distances requires terms accurate up to the tenth order.

Keywords: particle, bubble, ultrasound wave

PACS: 43.35.+d, 43.25.+y, 47.55.dp **DOI:** 10.1088/1674-1056/26/11/114303

1. Introduction

Many theoretical works have described the interaction between two or many gas bubbles in liquid.[1–15] In the present work, the theoretical framework of the model of bubble–bubble interaction[9] is applied to describe the interaction between a particle and an oscillating bubble driven by ultrasound waves in liquid. Both the particle and the bubble are free to translate.

The purpose of our study is motivated by a desire to account for the interaction between kidney stone fragments and cavitation clusters produced during shock wave lithotripsy.[16] However, the conditions of lithotripsy are complex. Thus, we consider a simple system with a suspended particle and a gas bubble under the condition that the liquid may be assumed as an ideal liquid.

There currently exist several studies on the interaction between bubbles and particles. Maxwell *et al.*[17] applied a three-dimensional discrete element method (DEM) to analyze the kinetics of collision of multiple particles against a stationary bubble and found that under this model the smaller particles were attracted more rapidly than the larger particles in the distribution. Mizushima *et al.*[18] found that an acoustic-cavitation-oriented bubble adhered to the particle and the particles moved toward the pressure anti-nodes of the standing wave in a kHz-order-ultrasound-irradiated water. Li *et al.*[19] demonstrated that the micron-size bubbles frosted on the solid surface can enhance the bubble–solid attachment. Vazirizadeh *et al.*[20] demonstrated coalescence and bubble–particle attachment are the main mechanisms explaining how the presence of solids affect the ties between the bubble size and gas hold-up. Zhang *et al.*[21] found that the particles can be accelerated by the collapsing bubbles up to 40 m/s and also be possibly split up by the cavitation in silt-laden flow.

The present research on fine particles and micro-size bubbles are mostly experiments. Most of the existing nonlinear models assume that the radii of the bubble and particle are large. Hay *et al.*[22] applied Lagrangian mechanics to derive a model of coupled pulsation and translation of a gas bubble and rigid particle and the accuracy of the model was higher than the fifth order. The analytical model with movable bubble and particle centers are valid for low amplitude spherical oscillations. Li *et al.*[23] used boundary integral method and experiments to study the interaction between a gas bubble and a suspended sphere.

It is thus an interesting idea to develop a theoretical model for nonlinear spherical pulsations and translational motions of an interacting particle and bubble that is valid to arbitrary distances between the particle and bubble, i.e., to remove the restriction that the distance of the particle and bubble is large.

2. Theory

Consider one spherical bubble and a rigid sphere surrounded by an ideal liquid and undergoing radial pulsations and translational motions. The geometry of the system is

*Project supported by the National Natural Science Foundation of China (Grant Nos. 11204168 and 11474191) and the Fundamental Research Funds for the Central Universities of China (Grant No. GK201603102).

†Corresponding author. E-mail: Wangld001@snnu.edu.cn

© 2017 Chinese Physical Society and IOP Publishing Ltd

presented in Fig. 1, where two local spherical coordinates $((r_j,\theta_j),\ (j=1,2))$ originate at the centers of the bubble and particle. The instantaneous radius of the bubble is given by $R_1(t)$, while the radius of the particle is fixed at R_2. $z_j(t)$ $(j=1,2)$ is the position of the center of the bubble and particle on the z axis measured from the center of bubble 1 at $t=0$.

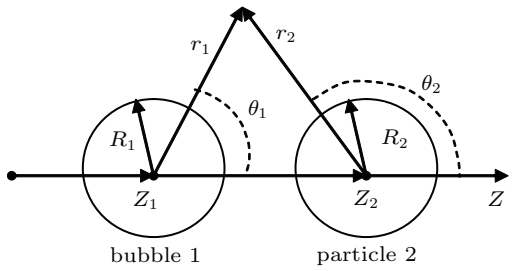


Fig. 1. Geometry of the system.

2.1. The velocity potential

In order to simplify the problem, the liquid is assumed to be incompressible, the flow is irritational, and the bubble keeps the spherical shape. The motion of the liquid surrounding the bubble and particle obeys Laplace's equation

$$\nabla^2\varphi_{\rm l}=0, \tag{1}$$

where $\varphi_{\rm l}$ is the velocity potential. Based on the linearity of Eq. (1), the total velocity potential $\varphi_{\rm l}$ can be expressed as

$$\varphi_{\rm l}=\varphi_1+\varphi_2, \tag{2}$$

where φ_1 and φ_2 are the velocity potentials of the bubble and particle. The expressions of φ_1 and φ_2 can be shown as follows:[1]

$$\varphi_1 = \sum_{n=0}^{\infty} a_{1n}\left(\frac{R_1}{r_1}\right)^{n+1} P_n(\cos\theta_1) \tag{3a}$$

$$= \sum_{n=0}^{\infty} b_{1n}\left(\frac{r_2}{d}\right)^{n} P_n(\cos\theta_2), \tag{3b}$$

$$\varphi_2 = \sum_{n=0}^{\infty} a_{2n}\left(\frac{R_2}{r_2}\right)^{n+1} P_n(\cos\theta_2) \tag{4a}$$

$$= \sum_{n=0}^{\infty} b_{2n}\left(\frac{r_1}{d}\right)^{n} P_n(\cos\theta_1), \tag{4b}$$

where P_n is the Legendre polynomial, $d(t)$ is the distance between the bubble and the particle, and $a_{1n}(t)$, $b_{1n}(t)$, $a_{2n}(t)$, and $b_{2n}(t)$ can be solved by the boundary conditions. Equation (3a) represents φ_1 in the coordinates of the bubble, and equation (3b) gives φ_1 in the coordinates of the particle. The potential φ_2 is similar to φ_1.

To solve Eqs. (3a)–(4b), the following mathematical identities can be used:[1]

$$\frac{P_n(\cos\theta_1)}{r_1^{n+1}} = \frac{1}{d^{n+1}}\sum_{\rm m=0}^{\infty}(-1)^m C_{nm}\left(\frac{r_2}{d}\right)^m P_m(\cos\theta_2), \tag{5a}$$

$$\frac{P_n(\cos\theta_2)}{r_2^{n+1}} = \frac{(-1)^n}{d^{n+1}}\sum_{\rm m=0}^{\infty} C_{nm}\left(\frac{r_1}{d}\right)^m P_m(\cos\theta_1), \tag{5b}$$

where $C_{nm}=(n+m)!/(n!m!)$. Substitution of Eq. (5a) into Eq. (3a) and Eq. (5b) into Eq. (4a) and comparison of the resulting expressions with Eqs. (3b) and (4b), respectively, yield

$$b_{1n}=(-1)^n\sum_{\rm m=0}^{\infty} C_{nm}\xi_1^{m+1}a_{1m}, \tag{6}$$

$$b_{2n}=\sum_{\rm m=0}^{\infty}(-1)^m C_{nm}\xi_2^{m+1}a_{2m},\quad \xi_j=R_j/d,\ j=1,2. \tag{7}$$

The time functions $a_{1n}(t)$ and $a_{2n}(t)$ are determined by the velocity boundary conditions

$$\frac{\partial\varphi_{\rm l}}{\partial r_1}=\dot R_1+\dot z_1\cos\theta_1,\quad \text{at}\quad r_1=R_1, \tag{8a}$$

$$\frac{\partial\varphi_{\rm l}}{\partial r_2}=\dot z_2\cos\theta_2,\quad \text{at}\quad r_2=R_2, \tag{8b}$$

where $\dot R_1$ represents the bubble pulsation, and $\dot z_j\cos\theta_j$ $(j=1,2)$ accounts for the translation of the particle and bubble.

With Eqs. (3a) and (4b), the velocity potential surrounding the bubble is expressed as

$$\varphi_{\rm l}=\sum_{n=0}^{\infty}\left[a_{1n}\left(\frac{R_1}{r_1}\right)^{n+1}+b_{2n}\left(\frac{r_1}{d}\right)^{n}\right]P_n(\cos\theta_1). \tag{9}$$

Substituting Eq. (9) into Eq. (8a) and replacing b_{2n} by a_{2m}, one obtains

$$a_{1n} = -R_1\dot R_1\delta_{n0}-\frac{R_1\dot z_1\delta_{n1}}{2} + \frac{n}{n+1}\xi_1^n\sum_{\rm m=0}^{\infty}(-1)^m C_{nm}\xi_2^{m+1}a_{2m}, \tag{10}$$

where δ_{nm} represents the Kronecker delta. Performing similar calculations for the particle, one obtains

$$\varphi_{\rm l}=\sum_{n=0}^{\infty}\left[a_{2n}\left(\frac{R_2}{r_2}\right)^{n+1}+b_{1n}\left(\frac{r_2}{d}\right)^{n}\right]P_n(\cos\theta_2), \tag{11}$$

$$a_{2n}=-\frac{R_2\dot z_2\delta_{n1}}{2}+\frac{(-1)^n n}{n+1}\xi_2^n\sum_{\rm m=0}^{\infty}C_{nm}\xi_1^{m+1}a_{1m}. \tag{12}$$

Substituting Eq. (12) into Eq. (10), one obtains

$$a_{1n}-\xi_1^n\sum_{k=0}^{\infty}\sum_{m=1}^{\infty}D_{nkm}^{(1)}a_{1k}\xi_1^{k+1}\xi_2^{2m+1} = -R_1\dot R_1\delta_{n0}-\frac{R_1\dot z_1\delta_{n1}}{2}+\frac{nR_2\dot z_2}{2}\xi_1^n\xi_2^2, \tag{13}$$

where

$$D_{nkm}^{(1)}=\frac{nmC_{nm}C_{mk}}{(n+1)(m+1)}. \tag{14}$$

The structure of Eq. (13) can be shown to have the following form:

$$a_{1n} = \sum_{l,s=0}^{\infty} \xi_1^l \xi_2^s \Big[-R_1 \dot{R}_1 \xi_1^n \alpha_{nls}^{(1)} - \frac{R_1 \dot{z}_1}{2} \xi_1^{n-1} \beta_{nls}^{(1)} + \frac{R_2 \dot{z}_2}{2} \xi_1^n \xi_2^2 \varepsilon_{nls}^{(1)} \Big], \tag{15}$$

where $\alpha_{nls}^{(1)}$, $\beta_{nls}^{(1)}$, and $\varepsilon_{nls}^{(1)}$ are unknown constants. Substituting Eq. (13) into Eq. (15) yields the following equations:

$$\sum_{l,s=0}^{\infty} \alpha_{nls}^{(1)} \xi_1^l \xi_2^s - \sum_{k=0}^{\infty} \sum_{m=1}^{\infty} \sum_{p,q=0}^{\infty} D_{nkm}^{(1)} \alpha_{kpq}^{(1)} \xi_1^{p+2k+1} \xi_2^{q+2m+1} = \delta_{n0}, \tag{16}$$

$$\sum_{l,s=0}^{\infty} \beta_{nls}^{(1)} \xi_1^l \xi_2^s - \sum_{k=0}^{\infty} \sum_{m=1}^{\infty} \sum_{p,q=0}^{\infty} D_{nkm}^{(1)} \beta_{kpq}^{(1)} \xi_1^{p+2k+1} \xi_2^{q+2m+1} = \delta_{n1}, \tag{17}$$

$$\sum_{l,s=0}^{\infty} \varepsilon_{nls}^{(1)} \xi_1^l \xi_2^s - \sum_{k=0}^{\infty} \sum_{m=1}^{\infty} \sum_{p,q=0}^{\infty} D_{nkm}^{(1)} \varepsilon_{kpq}^{(1)} \xi_1^{p+2k+1} \xi_2^{q+2m+1} = n. \tag{18}$$

Comparing the same power of ξ_1 and ξ_2 in Eqs. (16)–(18), one finds

$$\alpha_{0ls}^{(1)} = 0 \text{ except } \alpha_{000}^{(1)} = 1, \ \alpha_{nls}^{(1)} = 0 \text{ for } n \geq 1 \text{ if } l = 0 \text{ or } s < 3, \tag{19}$$

$$\alpha_{nls}^{(1)} = \sum_{k=0}^{[(l-1)/2]} \sum_{m=1}^{[(s-1)/2]} D_{nkm}^{(1)} \alpha_{k(l-2k-1)(s-2m-1)}^{(1)} \text{ for } n \geq 1, \ l \geq 1, \ s \geq 3, \tag{20}$$

$$\beta_{0ls}^{(1)} = 0, \ \beta_{nls}^{(1)} = 0 \text{ for } n \geq 1 \text{ if } l = 0 \text{ or } s < 3 \text{ eccept } \beta_{100}^{(1)} = 1, \tag{21}$$

$$\beta_{nls}^{(1)} = \sum_{k=0}^{[(l-1)/2]} \sum_{m=1}^{[(s-1)/2]} D_{nkm}^{(1)} \beta_{k(l-2k-1)(s-2m-1)}^{(1)} \text{ for } n \geq 1, \ l \geq 1, \ s \geq 3, \tag{22}$$

$$\varepsilon_{0ls}^{(1)} = 0, \ \varepsilon_{nls}^{(1)} = 0 \text{ for } n \geq 1 \text{ if } l = 0 \text{ or } s < 3 \text{ except } \varepsilon_{n00}^{(1)} = n, \tag{23}$$

$$\varepsilon_{nls}^{(1)} = \sum_{k=0}^{[(l-1)/2]} \sum_{m=1}^{[(s-1)/2]} D_{nkm}^{(1)} \varepsilon_{k(l-2k-1)(s-2m-1)}^{(1)} \text{ for } n \geq 1, \ l \geq 1, \ s \geq 3, \tag{24}$$

where $[x]$ means the integer part of x.

Performing similar calculation for a_{2n}, one obtains

$$a_{2n} = \sum_{l,s=0}^{\infty} \xi_2^l \xi_1^s \Big[-\frac{R_2 \dot{z}_2}{2} \xi_2^{n-1} \beta_{nls}^{(2)} - R_1 \dot{R}_1 \xi_2^n \xi_1 \gamma_{nls}^{(2)} - \frac{R_1 \dot{z}_1}{2} \xi_2^n \xi_1^2 \varepsilon_{nls}^{(2)} \Big], \tag{25}$$

$$\beta_{0ls}^{(2)} = 0, \ \beta_{nls}^{(2)} = 0 \text{ for } n \geq 1 \text{ if } l = 0 \text{ or } s < 3 \text{ eccept } \beta_{100}^{(2)} = 1, \tag{26}$$

$$\beta_{nls}^{(2)} = \sum_{k=0}^{[(l-1)/2]} \sum_{m=1}^{[(s-1)/2]} D_{nkm}^{(1)} \beta_{k(l-2k-1)(s-2m-1)}^{(1)} \text{ for } n \geq 1, \ l \geq 1, \ s \geq 3, \tag{27}$$

$$\gamma_{0ls}^{(2)} = 0, \ \gamma_{nls}^{(2)} = 0 \text{ for } n \geq 1 \text{ if } l = 0 \text{ or } s < 3 \text{ except } \gamma_{n00}^{(2)} = \frac{(-1)^n n}{n+1}, \tag{28}$$

$$\gamma_{nls}^{(2)} = \sum_{k=0}^{[(l-1)/2]} \sum_{m=1}^{[(s-1)/2]} D_{nkm}^{(1)} \gamma_{k(l-2k-1)(s-2m-1)}^{(2)} \text{ for } n \geq 1, \ l \geq 1, \ s \geq 3, \tag{29}$$

$$\varepsilon_{0ls}^{(2)} = 0, \ \varepsilon_{nls}^{(2)} = 0 \text{ for } n \geq 1 \text{ if } l = 0 \text{ or } s < 3 \text{ except } \varepsilon_{n00}^{(2)} = (-1)^n n, \tag{30}$$

$$\varepsilon_{nls}^{(2)} = \sum_{k=0}^{[(l-1)/2]} \sum_{m=1}^{[(s-1)/2]} D_{nkm}^{(1)} \varepsilon_{k(l-2k-1)(s-2m-1)}^{(2)} \text{ for } n \geq 1, \ l \geq 1, \ s \geq 3, \tag{31}$$

where

$$D_{nkm}^{(2)} = \frac{(-1)^{n+k} nm C_{nm} C_{mk}}{(n+1)(m+1)}. \tag{32}$$

2.2. Equations of motion

The equations of motion are derived using the Lagrange's equations, and they can be expressed as

$$\frac{\mathrm{d}}{\mathrm{d}t}\left(\frac{\partial L}{\partial \dot{R}_1}\right) = \frac{\partial L}{\partial R_1}, \frac{\mathrm{d}}{\mathrm{d}t}\left(\frac{\partial L}{\partial \dot{z}_j}\right) = \frac{\partial L}{\partial z_j}, \tag{33}$$

where dots over variables denotes time derivatives, and $L = T - U$, T is the kinetic energy, and U is the potential energy of the system.

The motion of the liquid surrounding the bubble, the particle, and the gas inside the bubble all contribute to the kinetic energy of the system, but the gas density is much lower than the liquid density, so the contribution of the gas may be ignored. The particle density is significant, and the kinetic energy associated with the translational motion of the particle (T_p) must be taken into account. Thus the total kinetic energy is

$$T = T_\mathrm{l} + T_\mathrm{p}, \tag{34}$$

where T_l is the liquid kinetic energy. The particle kinetic energy is simply

$$T_\mathrm{p} = \frac{1}{2} m_2 \dot{z}_2^2 = \frac{2}{3} \pi \rho_\mathrm{s} R_2^3 \dot{z}_2^2, \tag{35}$$

where m_2 is the mass of the suspended particle, and ρ_s is the particle density.

The kinetic energy of the liquid is calculated as

$$T_\mathrm{l} = \frac{\rho_\mathrm{l}}{2} \int_V (\nabla \varphi_\mathrm{l})^2 dV = \frac{\rho_\mathrm{l}}{2} \int_V \nabla \cdot (\varphi_\mathrm{l} \nabla \varphi_\mathrm{l}) \mathrm{d}V, \tag{36}$$

where V is the volume surrounding the particle and bubble, and ρ_l is the liquid density. Using Eqs. (8a) and (8b), the integrating over V can be rewritten as

$$T_\mathrm{l} = -\pi \rho_\mathrm{l} R_1^2 \int_0^\pi (\varphi_\mathrm{l})_{r_1 = R_1} \left(\dot{R}_1 + \dot{z}_1 \cos\theta_1\right) \sin\theta_1 \, \mathrm{d}\theta_1$$

$$-\pi\rho_{\rm l}R_2^2\int_0^{\pi}(\varphi_{\rm l})_{r_2=R_2}\dot{z}_2\cos\theta_2\sin\theta_2\,{\rm d}\theta_2. \tag{37}$$

Using Eqs. (9) and (11), one obtains

$$\begin{aligned}T_{\rm l} =& -2\pi\rho_{\rm l}\left[R_1^2\dot{R}_1\left(a_{10}+b_{20}\right)+\frac{R_1^2\dot{z}_1}{3}\left(a_{11}+b_{21}\xi_1\right)\right.\\&\left.+\frac{R_2^2\dot{z}_2}{3}\left(a_{21}+b_{11}\xi_2\right)\right].\end{aligned} \tag{38}$$

The potential energy of the system is expressed as follows:[6]

$$U=-\frac{4\pi}{3}R_1^3P_{\rm l}\left(t\right)-z_1F_{\rm D1}-z_2F_{\rm D2}, \tag{39}$$

where the scattered pressure at the surface of the bubble is expressed as $P_{\rm l}\left(t\right)$ and $F_{{\rm D}j}$ is the viscous drag force on the bubble and particle.

The Lagrangian function can be obtained by substituting Eqs. (15) and (25) into Eq. (38). It is expressed as follows:

$$\begin{aligned}L =& 2\pi\rho_{\rm l}\left[R_1^3\left(\dot{R}_1^2+\frac{\dot{z}_1^2}{6}\right)+R_2^3\frac{\dot{z}_2^2}{6}+L_{\rm int}\right]+\frac{1}{2}m_2\dot{z}_2^2\\&+\frac{4\pi}{3}R_1^3P_{\rm l}\left(t\right)+z_1F_{\rm D1}+z_2F_{\rm D2},\end{aligned} \tag{40}$$

where $L_{\rm int}$ represents the interaction between the bubble and particle, and it can be expressed as

$$\begin{aligned}L_{\rm int} =& R_1^3\left(\dot{R}_1^2f_1+\dot{R}_1\dot{z}_1f_3+\dot{z}_1^2f_4\right)+R_1^2R_2\left(\dot{R}_1\dot{z}_2f_2-\dot{z}_1\dot{z}_2f_5\right)\\&+R_2^3\dot{z}_2^2g_1+R_1R_2^2\left(\dot{R}_1\dot{z}_2g_2+\dot{z}_1\dot{z}g_3\right).\end{aligned} \tag{41}$$

f_n and g_n are expressed as

$$f_1=\sum_{m,l,s=0}^{\infty}(-1)^m\gamma_{mls}^{(2)}\xi_1^{s+1}\xi_2^{l+2m+1}, \tag{42}$$

$$f_2=\frac{1}{2}\sum_{m,l,s=0}^{\infty}(-1)^m\beta_{mls}^{(2)}\xi_1^{s}\xi_2^{l+2m}, \tag{43}$$

$$\begin{aligned}f_3 =& \frac{1}{3}\sum_{l,s=0}^{\infty}\alpha_{1ls}^{(1)}\xi_1^{l+1}\xi_2^{s}+\sum_{m,l,s=0}^{\infty}(-1)^m\xi_1^{s+2}\xi_2^{2m+l+1}\\&\times\left[\frac{1}{2}\varepsilon_{mls}^{(2)}+\frac{m+1}{3}\gamma_{mls}^{(2)}\right],\end{aligned} \tag{44}$$

$$\begin{aligned}f_4 =& \frac{1}{6}\sum_{\substack{l=1\\s=0}}^{\infty}\beta_{1ls}^{(1)}\xi_1^{l}\xi_2^{s}\\&+\frac{1}{6}\sum_{m,l,s=0}^{\infty}(-1)^m\left(m+1\right)\varepsilon_{mls}^{(2)}\xi_1^{s+3}\xi_2^{l+2m+1},\end{aligned} \tag{45}$$

$$\begin{aligned}f_5 =& \frac{1}{6}\sum_{l,s=0}^{\infty}\varepsilon_{1ls}^{(1)}\xi_1^{l+1}\xi_2^{s+2}\\&-\frac{1}{6}\sum_{m,l,s=0}^{\infty}(-1)^m\left(m+1\right)\beta_{mls}^{(2)}\xi_1^{s+1}\xi_2^{l+2m},\end{aligned} \tag{46}$$

$$g_1=\frac{1}{6}\sum_{\substack{l=1\\s=0}}^{\infty}\beta_{1ls}^{(2)}\xi_1^{s}\xi_2^{l}+\frac{1}{6}\sum_{m,l,s=0}^{\infty}(m+1)\varepsilon_{mls}^{(1)}\xi_1^{l+2m+1}\xi_2^{s+3}, \tag{47}$$

$$\begin{aligned}g_2 =& \frac{1}{3}\sum_{l,s=0}^{\infty}\gamma_{1ls}^{(2)}\xi_1^{s+1}\xi_2^{l+1}\\&-\frac{1}{3}\sum_{m,l,s=0}^{\infty}(m+1)\alpha_{mls}^{(1)}\xi_1^{l+2m+1}\xi_2^{s+1},\end{aligned} \tag{48}$$

$$\begin{aligned}g_3 =& \frac{1}{6}\sum_{l,s=0}^{\infty}\varepsilon_{1ls}^{(2)}\xi_1^{s+2}\xi_2^{l+1}\\&-\frac{1}{6}\sum_{m,l,s=0}^{\infty}(m+1)\beta_{mls}^{(1)}\xi_1^{l+2m}\xi_2^{s+1}.\end{aligned} \tag{49}$$

Substituting Eq. (40) into Eq. (33), one obtains three equations

$$R_1\ddot{R}_1+\frac{3}{2}\dot{R}_1^2-\frac{\dot{z}_1^2}{4}-\frac{P_{\rm l}}{\rho_{\rm l}}=G_1, \tag{50}$$

$$\frac{1}{3}R_1\ddot{z}_1+\dot{R}_1\dot{z}_1-\frac{F_{\rm D1}}{2\pi\rho_{\rm l}R_1^2}=H_1, \tag{51}$$

$$\frac{1}{3}R_2\left(1+\frac{2\rho_{\rm s}}{\rho_{\rm l}}\right)\ddot{z}_2-\frac{F_{\rm D2}}{2\pi\rho_{\rm l}R_2^2}=H_2, \tag{52}$$

$$\begin{aligned}G_1 =& -\left(R_1\ddot{R}_1+\frac{3}{2}\dot{R}_1^2\right)f_1+\frac{3}{2}\dot{z}_1^2f_4\\&-\frac{R_2}{R_1}\dot{z}_1\dot{z}_2f_5-\frac{R_2}{2}\left(\ddot{z}_2f_2+\dot{z}_2\dot{f}_2\right)\\&+\frac{1}{2}\left(\frac{R_2}{R_1}\right)^2\left(\dot{z}_1\dot{z}_2g_3-R_1\ddot{z}_2g_2-R_1\dot{z}_2\dot{g}_2\right)\\&-\frac{R_1}{2}\left(\ddot{z}_1f_3+\dot{z}_1\dot{f}_3+2\dot{R}_1\dot{f}_1\right),\end{aligned} \tag{53}$$

$$\begin{aligned}H_1 =& -\left(2R_1\ddot{z}_1+6\dot{R}_1\dot{z}_1\right)f_4-3\dot{R}_1^2f_3\\&-R_1\left(\ddot{R}_1f_3+\dot{R}_1\dot{f}_3+2\dot{z}_1\dot{f}_4\right)\\&-R_2\left(-\ddot{z}_2f_5-\dot{z}_2\dot{f}_5\right)+\frac{2R_2}{R_1}\dot{R}_1\dot{z}_2f_5\\&-\left(\frac{R_2}{R_1}\right)^2\left(\dot{R}_1\dot{z}_2g_3+R_1\ddot{z}_2g_3+R_1\dot{z}_2\dot{g}_3\right),\end{aligned} \tag{54}$$

$$\begin{aligned}H_2 =& -2R_2\ddot{z}_2g_1-\dot{R}_1^2g_2-\dot{R}_1\dot{z}_1g_3-2R_2\dot{z}_2\dot{g}_1\\&-R_1\left(\ddot{R}_1g_2+\dot{R}_1\dot{g}_2+\ddot{z}_1g_3+\dot{z}_1\dot{g}_3\right)\\&-\frac{2R_1}{R_2}\left(\dot{R}_1^2f_2-\dot{R}_1\dot{z}_1f_5\right)\\&-\left(\frac{R_1}{R_2}\right)^2\left(R_2\ddot{R}_1f_2+R_2\dot{R}_1\dot{f}_2-R_2\ddot{z}_1f_5-R_2\dot{z}_1\dot{f}_5\right).\end{aligned} \tag{55}$$

The expressions of G_1 and H_j are shown in the appendix.

The pressure $P_{\rm l}$ and the viscous drag force are shown in Refs. [9], [24], and [25] to be given by

$$\begin{aligned}P_{\rm l} =& P_{\rm G1}\left(\frac{R_{10}}{R_1}\right)^{3\gamma}\left(1-\frac{3\gamma\dot{R}_1}{c}\right)\\&-\frac{4\eta_{\rm l}\dot{R}_1}{R_1}-\frac{2\sigma_{\rm l}}{R_1}-P_0-P_{\rm ac},\end{aligned} \tag{56}$$

$$F_{{\rm D}j}=-12\pi\eta_{\rm l}R_j\dot{z}_j, \tag{57}$$

where $P_{\rm G1}$ is the equilibrium gas pressure inside the bubble, R_{10} is the equilibrium radius of the bubble, c is the speed of sound in the liquid, γ is the ratio of specific heats of the gas, $\sigma_{\rm l}$ is the surface tension, $\eta_{\rm l}$ is the dynamic viscosity of the liquid, P_0 is the hydrostatic pressure in the liquid, and $P_{\rm ac}$ is the driving acoustic pressure.

3. Numerical simulations

The nonlinear interaction between a particle and an oscillating bubble is studied using Lagrangian formalism, and one obtains a system of three coupled ordinary differential equations. One of them describes the radial oscillations of the bubble and the others describe the translation of the particle and bubble in liquid. The simulations of the system are carried out by the program package MATHEMATICA. It is assumed that the initial bubble radius is $R_1(0) = 1.5$ μm, the parameters of the gas inside the bubble and the surrounding liquid are $\rho_l = 998$ kg/m^3, $\eta_l = 0.001$ Pas, $\sigma_l = 0.072$ N/m, $c = 1482$ m/s, and $\gamma = 1.4$, and the ambient pressure is $P_0 = 101$ kPa. The simulations in this section show the high-order extensions of Eqs. (53)–(55) accurate to order $1/d^{10}$.

The instantaneous radius of the bubble and the time-varying distance between the bubble and the rigid sphere centers can be calculated using Eqs. (50)–(52). The result is presented in Fig. 2 which shows the different order in $1/d$. The equilibrium radii of the bubble and suspended particle are $R_{10} = 1.5$ μm and $R_{20} = 2.0$ μm, respectively. The initial separation distance between the particle and bubble is 10.5 μm and the sinusoidal acoustic pressure and frequency are 100 kPa and 1.7 MHz, respectively. The dashed curve shows the sum of the instantaneous bubble radius and the suspended particle radius, $R_1(t) + R_2$. The solid curves represent the separation distance between the particle and bubble, $d(t)$. The following observations can be reached. (i) Up to the fourth-order terms, the calculations predict repulsion between the particle and bubble. (ii) Beginning with the fifth order, the calculations predict attraction between the particle and bubble. During the bubble–particle coupling process, the phenomenon that the particle is pushed away by the expansion bubble and gets attracted towards the collapsing bubble is the same as Li's[23] experimental results. The translation line is more obvious when the numerical simulation is accurate to the tenth order. Therefore, the accuracy presented in the following figures is up to d^{-10}.

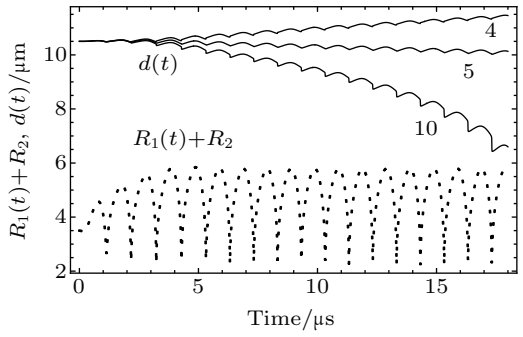


Fig. 2. The distance between the bubble and the rigid spherical sphere.

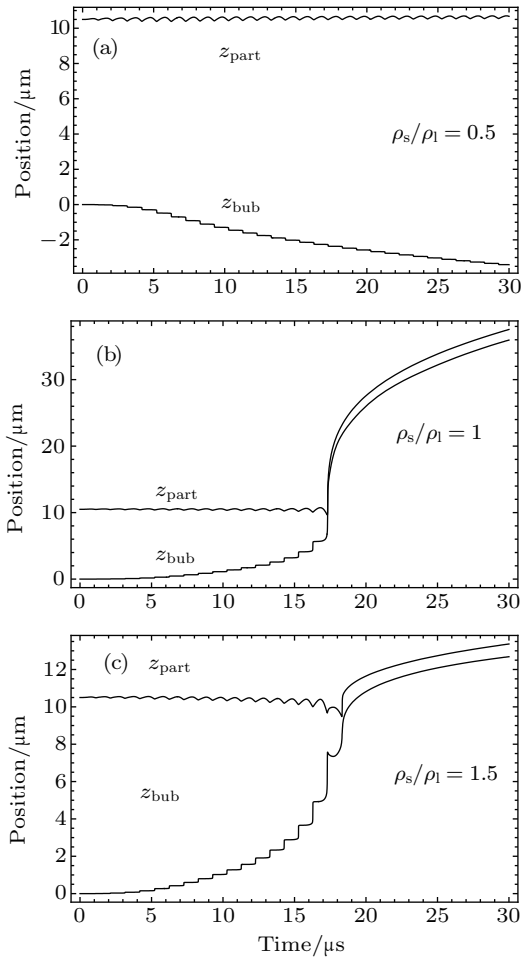


Fig. 3. Numerical solution of models accurate to order of $1/d^{10}$ for rigid particles of different densities. (a) Positions for a light particle ($\rho_s/\rho_l = 0.5$). (b) Positions for a neutral particle ($\rho_s/\rho_l = 1$). (c) Positions for a heavy particle ($\rho_s/\rho_l = 1.5$).

Figures 3(a)–3(c) show the positions and separation distances between the particle and bubble for three different particle densities ($\rho_s = 500$ kg/m^3, 998 kg/m^3, and 1500 kg/m^3). In this calculation, the equilibrium radius of the particle is set as $R_{20} = 2.0$ μm and the initial conditions for the positions are $z_1(0) = 0$ and $z_2(0) = 10.5$ μm, respectively. The bubble of equilibrium radius $R_{10} = 1.5$ μm is driven by an ultrasound wave of frequency 1.6 MHz and pressure amplitude 100 kPa. The simulations in this part are run with the tenth-order extensions of Eqs. (53)–(55). The results show that the attraction–repulsion between the particle and bubble is related to the particle densities. The following observations can easily be reached. (i) The time-averaged interaction between the particle and bubble repels for $\rho_s/\rho_l = 0.5$. (ii) The attraction between the particle and bubble is related to $\rho_s/\rho_l = 1.5$ and $\rho_s/\rho_l = 1$. (iii) The attraction between the particle and bubble is less after 18 μs, namely, the distance between them finally changes little over time. The result of the dependence on the particle densities is similar to Hay's theory,[24] which shows the initial separation distances (500 μm) between the particle and bubble for three density ratios ($\rho_s/\rho_l = 0.5, 1, 2$) when the sinusoidal acoustic pressure amplitude and frequency are

1 kPa and 32 kHz, respectively. Therefore it can be shown that our calculation is proper.

Figure 4(a) demonstrates the movement process of the bubble and particle via changing the bubble radii while the particle size ($R_{20} = 2.0$ μm) is kept unchanged. The driving frequency is 1.7 MHz, the other parameters are the same as those in Fig. 3. It shows that the attraction between light particle and bubble does not increase as the bubble size grows. There exists an optimal R_{10} (around 1.5 μm), which can maximize the interaction between the particle and bubble. Figure 4(b) demonstrates the case of increasing the particle size while keeping the bubble radius ($R_{10} = 2.0$ μm) unchanged. It is obvious that attraction forces between the particle and bubble do not increase with the increased particle size, but when the size of the particle is 3.0 μm, the interaction between them is relatively strong. Comparing with Fig. 3(a), the result shows that the decrease of the particle size not only leads to the attraction of the interaction between the light particle and bubble, but also makes it get smaller. The phenomenon is similar to Li's research,[23] if $\theta \to 0$ ($\theta = R_s/R_m$, where R_s is the sphere radius and R_m is the maximum equivalent bubble radius), the effect of sphere motion on bubble dynamics tends to none, and there also exists an optimal θ (around 2).

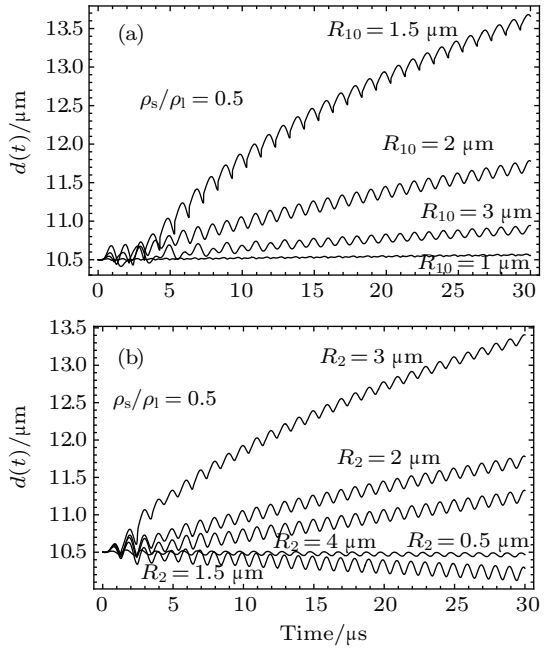


Fig. 4. (a) Response of bubble with initial radius of 1.5 μm, 2 μm, and 3 μm, respectively, and μight ($\rho_s/\rho_l = 0.5$) particle with initial radius 2 μm. (b) Response of light particle with initial radius of 1.5 μm, 2 μm, and 3 μm, respectively, and bubble with initial radius 2 μm.

The effect of the acoustic forcing on the attraction–repulsion between the particle and bubble is investigated, as shown in Fig. 5. It is assumed that the bubble and particle are driven by an ultrasound wave of pressure amplitude of 70 kPa, 100 kPa, and 130 kPa, respectively. The driving frequency is 1.7 MHz, and the other parameters are the same as those in Fig. 3. Figures 5(a) and 5(b) represent the two different particle densities: $\rho_s = 500$ kg/m^3 and 1500 kg/m^3. For a light ($\rho_s/\rho_l = 0.5$) particle, the repulsion increases with the increment of the acoustic forcing. Similarly for a rigid heavy ($\rho_s/\rho_l = 1.5$) particle, the increment of the time-averaged pressure makes the attraction between the bubble and particle stronger, particularly, the distance between the bubble and particle finally changes little over time. Namely, the separation distance between the bubble and heavy particle will reach a steady state.

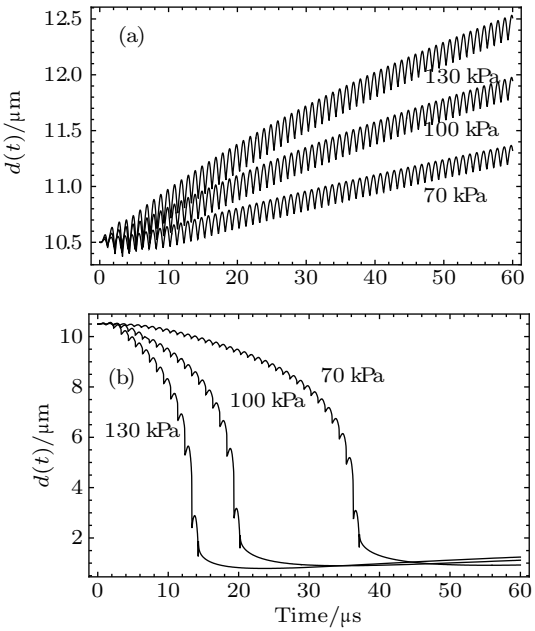


Fig. 5. (a) Response of three different acoustic forcing for a light particle ($\rho_s/\rho_l = 0.5$). (b) Response of three different acoustic forcing for a heavy particle ($\rho_s/\rho_l = 1.5$).

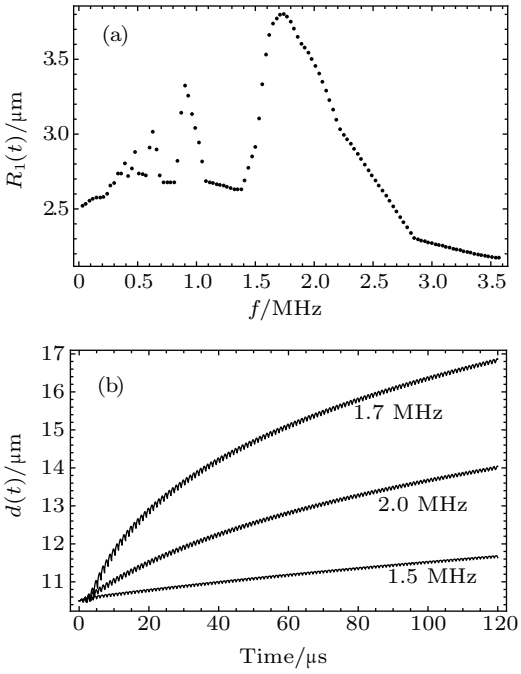


Fig. 6. (a) Resonance curves of the bubble. (b) Influence of different frequencies on the interaction between the particle and bubble.

The natural frequency (frequency of maximum response) of the bubble is shown in Fig. 6(a), and to get the estimated value of 1.71 MHz. Based on the natural frequency of the bubble, the influence of three frequencies ($f = 1.5$ MHz, 1.7 MHz, and 2.0 MHz) on the interaction between the bubble and particle is investigated, as shown in Fig. 6(b). The parameters are the same as those in Fig. 3. It is found that, with acoustic frequencies approaching the natural frequency, the repulsion of the bubble and the light particle greatly increases.

4. Summary

Lagrangian mechanics were used to derive dynamical equations describing the spherical pulsations and translational motions of interacting bubble and particle in an incompressible liquid. The model consists of three coupled ordinary differential equations. One of them describes the pulsation of the bubble and the other two describe the translation of the bubble and particle in an infinite, incompressible liquid. Dynamical models accurate to higher order of $1/d^{10}$ were generated via the program package MATHEMATICA. It has been found that the interaction between the bubble and particle is governed by four effects: the density and size of the particle and the driving acoustic pressure and frequency.

Appendix A: expression for G_1 and H_j

$$G_1 = \frac{G_1^{(2)}}{d^2} + \frac{G_1^{(3)}}{d^3} + \frac{G_1^{(4)}}{d^4} + \frac{G_1^{(5)}}{d^5} + \frac{G_1^{(6)}}{d^6} + \frac{G_1^{(7)}}{d^7} + \frac{G_1^{(8)}}{d^8} + \frac{G_1^{(9)}}{d^9} + \frac{G_1^{(10)}}{d^{10}}, \tag{A1}$$

$$G_1^{(2)} = \frac{1}{2}R_2^3\ddot{z}_2, \tag{A2}$$

$$G_1^{(3)} = -\frac{1}{2}R_2^3\dot{z}_2\left(\dot{z}_1 + 2\dot{z}_2\right), \tag{A3}$$

$$G_1^{(4)} = -\frac{1}{2}R_2^3R_1\left(2\dot{R}_1^2 + R_1\ddot{R}_1\right), \tag{A4}$$

$$G_1^{(5)} = -\frac{1}{2}R_2^3R_1^2\left[4\ddot{R}_1\left(\dot{z}_1 - \dot{z}_2\right) + R_1\ddot{z}_1\right], \tag{A5}$$

$$G_1^{(6)} = \frac{1}{12}R_2^3\left[-16R_2^2R_1\dot{R}_1^2 - 6R_1^3\dot{z}_1\left(2\dot{z}_1 - 5\dot{z}_2\right) + 9R_2^3\dot{z}_2^2 - 8R_2^2R_1^2\ddot{R}_1\right], \tag{A6}$$

$$G_1^{(7)} = -\frac{1}{6}R_2^5R_1^2\left[24\dot{R}_1\left(\dot{z}_1 - \dot{z}_2\right) + 5R_1\ddot{z}_1\right], \tag{A7}$$

$$G_1^{(8)} = \frac{1}{12}R_2^5R_1\left[-18R_2^2\dot{R}_1^2 + R_1\left(30R_2\dot{z}_2^2 - 9R_2^2\ddot{R}_1\right) + R_1^2\left(70\dot{z}_1\dot{z}_2 + 6R_2\ddot{z}_2 - 34\dot{z}_1^2\right)\right], \tag{A8}$$

$$G_1^{(9)} = -\frac{1}{4}R_2^6R_1^2\left[24R_2\dot{R}_1\left(\dot{z}_1 - \dot{z}_2\right) + R_1\left(16\dot{z}_2^2 + 5R_2\ddot{z}_1 - 4\dot{z}_1\dot{z}_2\right)\right], \tag{A9}$$

$$G_1^{(10)} = \frac{1}{4}R_2^6R_1^3\left[R_2\left(45\dot{z}_1\dot{z}_2 + 2R_2\ddot{z}_2 - 21\dot{z}_1^2\right) - 7R_1\left(\dot{R}_1^2 - 4\dot{z}_2^2\right) - 2R_1^2\left(\ddot{R}_1 - \ddot{z}_2\right)\right], \tag{A10}$$

$$H_1 = \frac{H_1^{(3)}}{d^3} + \frac{H_1^{(4)}}{d^4} + \frac{H_1^{(5)}}{d^5} + \frac{H_1^{(6)}}{d^6} + \frac{H_1^{(7)}}{d^7} + \frac{H_1^{(8)}}{d^8} + \frac{H_1^{(9)}}{d^9} + \frac{H_1^{(10)}}{d^{10}}, \tag{A11}$$

$$H_1^{(3)} = R_2^3\left(\dot{R}_1\dot{z}_2 + R_1\ddot{z}_2\right), \tag{A12}$$

$$H_1^{(4)} = -3R_1R_2^3\dot{z}_2^2, \tag{A13}$$

$$H_1^{(5)} = -R_2^3R_1^2\left(3\dot{R}_1^2 + R_1\ddot{R}_1\right), \tag{A14}$$

$$H_1^{(6)} = -R_2^3R_1^3\left[\dot{R}_1\left(6\dot{z}_1 - 5\dot{z}_2\right) + R_1\ddot{z}_1\right], \tag{A15}$$

$$H_1^{(7)} = \frac{1}{3}R_2^3R_1\left[9R_2^3\dot{z}_2^2 - 5R_2^2R_1^2\ddot{R}_1 - 13R_1R_2^2\dot{R}_1^2 - 9R_1^3\dot{z}_1\left(\dot{z}_1 - 2\dot{z}_2\right)\right], \tag{A16}$$

$$H_1^{(8)} = -\frac{1}{3}R_2^5R_1^3\left[\dot{R}_1\left(36\dot{z}_1 - 35\dot{z}_2\right) + 6R_1\ddot{z}_1\right], \tag{A17}$$

$$H_1^{(9)} = -\frac{1}{2}R_2^5R_1^2\left[13R_2^2\dot{R}_1^2 + R_2R_1\left(4\dot{R}_1\dot{z}_2 + 5R_2\ddot{R}_1 - 16\dot{z}_2^2\right) + 2R_1^2\left(8\dot{z}_1^2 - 16\dot{z}_1\dot{z}_2 - R_2\ddot{z}_2\right)\right], \tag{A18}$$

$$H_1^{(10)} = -\frac{1}{2}R_2^6R_1^3\left[\dot{R}_1\left(48R_2\dot{z}_1 - 45R_2\dot{z}_2\right) + 2R_1\left(9\dot{z}_2^2 + 4R_2\ddot{z}_1\right)\right], \tag{A19}$$

$$H_2 = \frac{H_2^{(2)}}{d^2} + \frac{H_2^{(3)}}{d^3} + \frac{H_2^{(4)}}{d^4} + \frac{H_2^{(5)}}{d^5} + \frac{H_2^{(6)}}{d^6} + \frac{H_2^{(7)}}{d^7} + \frac{H_2^{(8)}}{d^8} + \frac{H_2^{(9)}}{d^9} + \frac{H_2^{(10)}}{d^{10}}, \tag{A20}$$

$$H_2^{(2)} = R_2R_1\left(2\dot{R}_1^2 + R_1\ddot{R}_1\right), \tag{A21}$$

$$H_2^{(3)} = R_2R_1^2\left(5\dot{R}_1\dot{z}_1 + R_1\ddot{z}_1\right), \tag{A22}$$

$$H_2^{(4)} = 3R_2R_1^3\dot{z}_1^2, \tag{A23}$$

$$H_2^{(5)} = -2R_2R_1^4\dot{R}_1^2, \tag{A24}$$

$$H_2^{(6)} = -R_2R_1^2\left(5R_1^3\dot{R}_1\dot{z}_1 + 3R_2^3\dot{R}_1\dot{z}_2 + R_2^3R_1\ddot{z}_2\right), \tag{A25}$$

$$H_2^{(7)} = -R_2R_1^3\left[4R_2^2R_1\dot{R}_1^2 + 3R_1^3\dot{z}_1^2 + 3R_2^3\dot{z}_2\left(2\dot{z}_1 - \dot{z}_2\right)\right], \tag{A26}$$

$$H_2^{(8)} = \frac{1}{3}R_2^3R_1^4\left[15R_2\dot{R}_1^2 - 5\dot{R}_1\left(7R_1\dot{z}_1 + 6R_2\dot{z}_2\right) + 3R_2R_1\left(\ddot{R}_1 - 2\ddot{z}_2\right)\right], \tag{A27}$$

$$H_2^{(9)} = R_2^3R_1^4\left[-6R_2^2\dot{R}_1^2 + 14R_2R_1\dot{R}_1\dot{z}_1 + 8R_1R_2\dot{z}_2\left(-2\dot{z}_1 + \dot{z}_2\right) + R_1^2\left(-8\dot{z}_1^2 + R_2\ddot{z}_1\right)\right], \tag{A28}$$

$$H_2^{(10)} = \frac{1}{2}R_2^4R_1^4\left[2\dot{R}_1^2\left(5R_2^2 + 7R_1^2\right) - R_1\dot{R}_1\left(45R_2\dot{z}_1 + 56R_1\dot{z}_2\right) + 2R_1\left(9R_1\dot{z}_1^2 + R_2^2\ddot{R}_1\right) + 2R_1^3\left(\ddot{R}_1 - 4\ddot{z}_2\right)\right]. \tag{A29}$$

References

[1] Doinikov A A 2001 *Phys. Rev. E* **64** 026301
[2] Ida M 2003 *Phys. Rev. E* **67** 056617
[3] Doinikov A A 2004 *J. Acoust. Soc. Am.* **116** 821
[4] Hamilton M F, Ilinskii Y A, Meegan G D and Zabolotskaya E A 2005 *ARLO* **6** 207
[5] Ilinskii Y A, Hamilton M F and Zabolotskaya E A 2007 *J. Acoust. Soc. Am.* **121** 786
[6] Chew L W, Klaseboer E, Ohl S W and Khoo B C 2013 *Exp. Therm. Fluid Sci.* **44** 108
[7] Wang C H and Cheng J C 2013 *Chin. Phys. B* **22** 014304
[8] Zou J, Li B and Ji C 2015 *Exp. Therm. Fluid Sci.* **61** 105

[9] Doinikov A A and Bouakaz A 2015 *Phys. Rev. E* **92** 043001
[10] Han R, Zhang A and Liu Y L 2015 *Ocean. Eng.* **110** 325
[11] Daemi M, Rahni M T and Massah H 2015 *Chin. Phys. B* **24** 024302
[12] Li S and Ni B Y 2016 *Eng. Anal. Bound. Elem.* **68** 63
[13] Shi J, Yang D S, Shi S G, Hu B, Zhang H Y and Hu S Y 2016 *Chin. Phys. B* **25** 024304
[14] Gumnlya M, Utikar R P, Evans G M, Joshi J B and Pareek V 2017 *Chem. Eng. Sci.* **166** 1
[15] Liang J F, Wang X, Yang J and Gong L X 2017 *Ultrasonics* **75** 58
[16] Pishchalnikov Y A, Sapozhnikov O A, Bailey M R, Williams J C, Cleveland R O, Colonius T, Crum L A, Evan A P and McAteer J A 2003 *J. Endourol* **17** 435
[17] Maxwell R, Ata S, Wanless E J and Moreno-Atanasio R 2012 *J. Colloid Interface Sci.* **381** 1
[18] Mizushima Y, Nagami Y, Nakamara Y and Saito T 2013 *Chem. Eng. Sci.* **93** 395
[19] Li H P, Afacan A, Liu Q X and Xu Z H 2015 *Miner. Eng.* **84** 106
[20] Vazirizadeh A, Bouchard J and Chen Y 2016 *Int. J. Miner. Process.* **157** 163
[21] Zhang Y N, Qian Z D, Ji B and Wu Y L 2016 *Renew. Sust. Energ. Rev.* **56** 303
[22] Hay T A, Hamilton M F, Ilinskii Y A and Zabolotskaya E A 2009 *J. Acoust. Soc. Am.* **125** 1331
[23] Li S, Han R and Zhang A M 2016 *J. Fluids Struct.* **65** 333
[24] van der Meer S M, Dollet B, Voormolen M M, Chin C T, Bouakaz A, de Jong N, Versluis M and Lohse D 2007 *J. Acoust. Soc. Am.* **121** 648
[25] Magnaudet J and Legendre D 1998 *Phys. Fluids* **10** 550